Morphology of Rare-Earth Polymeric Electrolytes

M. M. S. Puga,[†,§] L. D. Carlos,*[,‡,§] T. M. A. Abrantes,[§] and L. Alcácer[§]

Microfabritech, University of Florida, Gainesville, Florida 32611; Departamento de Física, Universidade de Évora, AP 94, 7001 Évora Codex, Portugal; and Centre for Microsystems, Instituto Superior Técnico, 1096 Lisboa, Portugal

Received May 8, 1995. Revised Manuscript Received October 4, 1995[⊗]

The usual two-solvent casting technique was used to prepare a series of poly(ethylene oxide), PEO, and poly(propylene oxide), PPO, electrolytes containing trivalent salts of Eu, Nd, and Pr with concentrations between $n = 80$ and $n = 3$ (n is the number of ether oxygen atoms in the polymer chain per lanthanide cation). The films were characterized by differential scanning calorimetry, scanning electron microscopy/energy-dispersive X-ray microanalysis, and X-ray powder diffraction. The Eu^{3+} and Pr^{3+} electrolytes with $n \geq 8$ exhibit an endothermic peak around 65 °C, which is associated with the melting of crystalline PEO. Films with compositions $16 \geq n \geq 7$ showed, in addition, a smaller endotherm around 60 °C, which results from a eutectic phase of PEO and PEO/salt complex. The highly concentrated PEO_nEuBr_3 films, $n \leq 6$, are a glassy, transparent, and fragile materials when no traces of water are detected. The stoichiometry of the high-melting-point crystalline complex observed for these Eu^{3+} electrolytes appears to be close to an oxygen–cation ratio of 3:1. The morphology of the Nd^{3+} electrolytes was found to be independent of the salt concentration. These films are characterized by the presence of a crystalline PEO phase and, probably, a nonstoichiometric PEO–$NdCl_3$ complex. PPO–$EuBr_3$ electrolytes are predominantly amorphous and formation of a salt-rich complex phase was also observed at high salt concentrations.

Introduction

During the past two decades, complexes of high molecular weight polymers and metal salts have been extensively investigated as reported by several review papers.[1–3] The unique properties of these materials, which combine a plastic nature with ionic conductivity, makes them very promising for the development of thin-film rechargeable solid-state batteries, electrochromics, sensors, and microionic devices.[4]

It is well-known that high molecular weight poly(ethylene oxide), PEO, and poly(propylene oxide), PPO, can dissolve a wide range of ionic salts of monovalent, divalent, and trivalent cations to form ionically conducting solid polymer electrolytes.[5–7] Although monovalent- and divalent-salt-based polymer electrolytes have been extensively studied and are well documented,[4,8–18] only a limited amount of work has been reported on polymer electrolytes containing trivalent rare-earth cations.[19–32] The interest of these systems arises from the possibility

† University of Florida.
‡ Universidade de Évora.
§ Instituto Superior Técnico.
⊗ Abstract published in *Advance ACS Abstracts,* November 15, 1995.

(1) MacCallum, J. R., Vincent, C. A., Eds. *Polymer Electrolyte Reviews*; Elsevier Applied Science: London, 1987, 1989; Vol. 1, 2.
(2) Linford, R. G., Ed. *Electrochemical Science and Technology of Polymers*; Elsevier Applied Science: London, 1987.
(3) Scrosati, B., Ed. *Second International Symposium on Polymer Electrolytes*; Elsevier Applied Science: London, 1990.
(4) Vincent, C. A. *Prog. Solid State Chem.* **1987,** *17,* 189.
(5) Fenton, D. E.; Parker, J. M.; Wright, P. V. *Polymer* **1973,** *14,* 589.
(6) Armand, M. B.; Chabagno, J. B.; Duclot, M. *Fast Ion Transport in Solids*; Vashishta, P., Mundy, J. N., Shenoy, G. K., Eds.; North-Holland: Amsterdam, 1979; p 131.
(7) Farrington, G. C.; Linford, R. G. *Polymer Electrolyte Reviews 2*; MacCallum, J. R., Vincent, C. A., Eds.; Elsevier Applied Science: London, 1989; Chapter 8.
(8) Armand, M. B. *Solid State Ionics* **1983,** *9/10,* 745.
(9) Patrick, A.; Glasse, M. D.; Latham, R.; Linford, R. G. *Solid State Ionics* **1986,** *18/19,* 1063.
(10) Abrantes, T. M. A.; Alcácer, L.; Sequeira, C. A. C. *Solid State Ionics* **1986,** *18/19,* 315.
(11) Yang, H.; Huq, R.; Farrington, G. C. *Solid State Ionics* **1990,** *40/41,* 663.
(12) Einset, A. G.; Schlindwein, W. S.; Latham, R. J.; Linford, R. G. *J. Electrochem. Soc.* **1991,** *138,* 1569.
(13) Yang, H.; Farrington, G. C. *J. Electrochem. Soc.* **1992,** *139,* 1646.
(14) Yang, L. L.; McGhie, A. R.; Farrington, G. C. *J. Electrochem. Soc.* **1986,** *133,* 1380.
(15) Huq, R.; Chiodelli, G. C.; Ferloni, P.; Magistris, A.; Farrington, G. C. *J. Electrochem. Soc.* **1987,** *134,* 364.
(16) Huq, R.; Farrington, G. C. *J. Electrochem. Soc.* **1988,** *135,* 524.
(17) Cai, H.; Hu, R.; Egami, T.; Farrington, C. G. *Solid State Ionics* **1992,** *52,* 333.
(18) Pantaloni, S.; Passerini, S.; Scrosati, B. *J. Electrochem. Soc.* **1988,** *135,* 1951.
(19) Bruce, P. G.; Krok, F.; Nowinski, J.; Gray, F. M.; Vincent, C. A. *Mater. Sci. Forum* **1989,** *42,* 193.
(20) Huq, R.; Farrington, G. C. *Second International Symposium on Polymer Electrolytes*; Scrosati, B., Ed.; Elsevier Applied Science: London, 1990; p 273.
(21) Reis Machado, A. S.; Alcácer, L. *Second International Symposium on Polymer Electrolytes*; Scrosati, B., Ed.; Elsevier Applied Science: London, 1990; p 283.
(22) Silva, C. J.; Smith, M. J. *Solid State Ionics* **1992,** *58,* 269; **1993,** *60,* 73.
(23) Bernson, A.; Lindgren, J. *Solid State Ionics* **1993,** *60,* 31.
(24) Carlos, L. D.; Assunção, M.; Abrantes, T. M.; Alcácer, L. *Solid State Ionics III*; Nazri, G.-A., Tarrascon, J.-M.; Armand, M. B., Eds.; Mater. Res. Soc. Proc.; MRS: Pittsburgh, PA, 1993; Vol. 293, p 117.
(25) Carlos, L. D.; Videira, A. L. L. *Phys. Rev. B* **1994,** *49,* 11721.
(26) Brodin, A.; Mattsson, B.; Torell, L. M. *J. Chem. Phys.* **1994,** *101,* 4621.
(27) Carlos, L. D.; Videira, A. L. L. *J. Chem. Phys.* **1994,** *101,* 8827.
(28) Carlos, L. D.; Assunção, M.; Alcácer, L. *J. Mater. Res.* **1995,** *10,* 202.
(29) Carlos, L. D.; Videira, A. L. L.; Assunção, M.; Alcácer, L. *Electrochim. Acta* **1995,** *40,* 2143.
(30) Carlos, L. D.; Assunção, M.; Alcácer, L. *Synth. Met.* **1995,** *69,* 587.
(31) Carlos, L. D.; Assunção, M., to be published.

0897-4756/95/2807-2316$09.00/0

of combining the luminescent emission of the lanthanide cations with the material advantages of processible plastic films with variable thickness and large surface areas. Indeed, these polymer electrolytes are strongly luminescent from 14 K to room temperature with lifetimes on the order of 1 ms at low temperatures.[24-31] We believe that these unique properties will certainly open new prospects for technological applications of polymer electrolytes in the electronic, optoelectronic, and even medical-pharmaceutical domains. In addition, the luminescence features of Eu^{3+}-based electrolytes can shed further insight on the local structure surrounding the cation in the PEO and PPO matrices.[25-29]

In the present work, differential scanning calorimetry (DSC), scanning electron microscopy/energy-dispersive X-ray microanalysis (SEM/EDX), and X-ray powder diffraction (XRD) were used to analyze phase transitions, morphology, and salt distribution in a series of PEO complexes of Eu, Nd, and Pr halides with compositions between $n = 80$ and $n = 3$, with n being the number of ether oxygen atoms in the polymeric chain per lanthanide cation. Similar analysis were carried out for selected compositions of PPO_nEuBr_3 electrolytes, $n = 32,20,8$.

Experimental Section

Sample Preparation. A two-solvent solution casting technique was used to prepare the polymer electrolyte films. PEO (molecular weight of 5×10^6, Aldrich) was dried under vacuum at 60 °C for 3 days prior to sample preparation. Stoichiometric amounts of ultrapure $EuBr_3$, $NdCl_3$, and $PrCl_3$ salts and PEO were dissolved in ethanol–acetonitrile mixtures and then cast. The resulting polymer films were vacuum dried first at room temperature for about 48 h, then at 70 °C for another 24 h, and finally at room temperature for an additional 5 days. The dried polymer films were stored in an Ar-atmosphere drybox and all subsequent handling was performed in dry conditions. The same process was used for the preparation of PPO (molecular weight of 5×10^7, Zeon Chemicals) with $EuBr_3$ salt.

The compositions studied in this work were PEO_nEuBr_3 where n varies from 80 to 3, PPO_nEuBr_3 with $n = 32$, 20, 8, PEO_nPrCl_3 where n varies from 40 to 8, and PEO_nNdCl_3 where n varies from 40 to 3. It should be mentioned that although preparation of Pr^{3+} highly concentrated compositions, $n < 8$, were attempted, no homogeneous films could be obtained, probably due to a salting-out effect.

Sample Characterization. DSC analysis were performed with a Mettler FP800. The microstructures were analysed with a polarized optical microscope Labophot 2-Pol Nikon PFX equipped with a Mettler FP 84 TA microscopy cell and a Nikon FX-35W camera. All DSC analysis were carried out under a flow of Ar. The heating rate was varied between 10 and 5 °C/min. Two heating cycles were done for each film. The films were first heated from room temperature to 200 °C, then cooled to room temperature, and immediately reheated to 270–300 °C.

The SEM/EDX studies were performed using an SEM JEOL JSM 6400 coupled with a Tracor Northern series II X-ray Microanalysis system. The primary electron beam energy was varied between 2, 5, and 10 keV in order to minimize beam-induced damage. X-ray microanalysis was carried out at an accelerating voltage of 10 and 15 keV. The samples were mounted in small carbon stubs with carbon paint and evaporation-coated with a thin carbon layer in order to provide a conducting surface and minimize electron-beam-induced damage.

XRD analysis was carried out with a Phillips PW-1010 diffractometer using Cu Kα radiation. Samples for X-ray powder diffraction were prepared by grinding under liquid N_2 for about 20 min. The resulting polymer electrolyte powders were then sealed in Lindaman tubes and heated at 120–130 °C for 4 days and then kept at 60 °C for an additional 4 days and at room temperature for another 4 days.

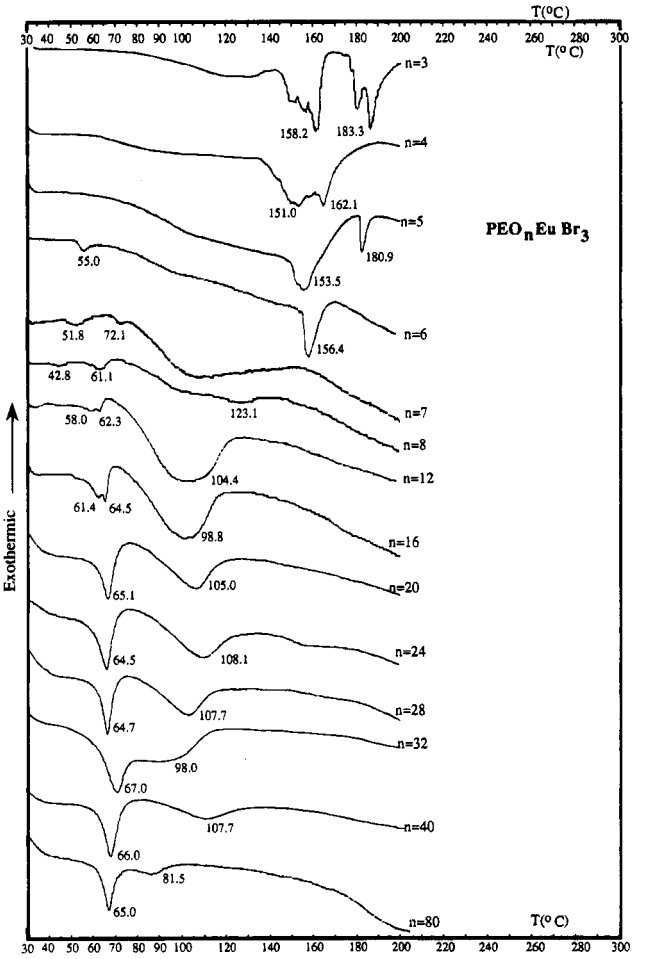

Figure 1. DSC curves for the first heating cycle of the system PEO_nEuBr_3 with n ranging from 80 to 3. (Films with $n \geq 20$ were run at 10 °C/min and films with $n \leq 16$ were run at 5 °C/min).

Results and Discussion

PEO– and PPO–$EuBr_3$ Systems. Figure 1 shows the DSC curves obtained during the first heating cycle of the system PEO_nEuBr_3 with n ranging from 80 to 3. The electrolyte films with compositions $80 \geq n \geq 20$ undergo a melting transition that occurs at a well-defined temperature and is characterized by a sharp first endothermic peak. The temperature of the first endotherm is close to the temperature of the melting point of pure PEO (65 °C),[1-3] which indicates that the crystalline phase of the films consists mostly of uncomplexed crystalline PEO. With increasing salt concentrations, the peak shifts to lower temperatures due to dissolved ions being accommodated in the crystalline PEO phase.[17]

Salt-rich films with compositions $16 \geq n \geq 7$ display, in addition, a smaller endothermic peak adjacent to the PEO melting endotherm. This smaller peak did not occur upon reheating. Therefore, it is reasonable to assume from the DSC data that it results from the eutectic phase of a PEO–PEO/salt complex. These results indicate that the eutectic composition lies within $12 > n \geq 8$. A melting temperature depression caused

(32) Puga, M. M. S.; Carlos, L. D.; Abrantes, T. M.; Alcácer, L. *Electrochim. Acta* **1995**, *40*, 2383.

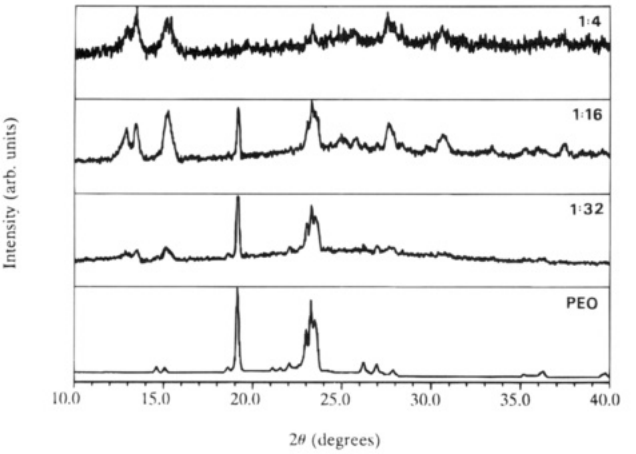

Figure 2. X-ray powder diffraction pattern of pure PEO and PEO_nEuBr_3 with $n = 32$, 16, 4.

by the formation of an eutectic phase has been reported for other PEO−rare-earth salt systems.[20,22]

For the highly concentrated films, $n \leq 6$, no crystalline PEO and eutectic phases were detected. The DSC data show instead endothermic peaks around 150 °C, which corresponds to the melting of a stoichiometric crystalline salt−polymer complex.[16,17] This complex starts to decompose at ≈140 °C, becoming liquid at first. Actually, it can be observed to boil off under the optical microscope. This is illustrated in the DSC curves (Figure 1) as irregular peaks in the temperature region 140−190 °C. The stoichiometry of this crystalline complex appears to be close to an oxygen−cation ratio of 3:1. The existence of a high-melting-point crystalline complex with a stoichiometry 4:1 or 3:1 was previously suggested for trivalent-cation-based PEO electrolytes,[33] although this is the first time it has ever been observed. These results are further supported by X-ray analysis and microscopy studies.

Figure 2 shows the XRD patterns of pure PEO and PEO_nEuBr_3 (with $n = 32$, 16, and 4) at room temperature. The Bragg peaks resulting from pure PEO are well-defined. The diffraction pattern of the electrolyte with low salt concentration, $n = 32$, is basically identical with that of pure PEO. However, with increasing salt concentration, the intensities of the peaks due to the pure PEO crystalline phase decrease and disappear for the film $n = 4$ as more salt is being incorporated in the PEO crystalline phase. These results correlate well with the DSC data (Figure 1). Although the XRD pattern of film $n = 4$ is ill-defined at room temperature, it exhibits peaks from a crystalline complex.

From the DSC data (Figure 1) a broad endotherm peak is seen above the melting PEO for electrolytes with compositions in the range $80 \geq n \geq 12$. This endotherm may be presumably due to the loss of water eventually adsorbed during the transference of the samples from the glovebox, which is consistent with the fact that Eu-complexes are usually highly hygroscopic.[20] However, it has been reported for PEO-based Zn^{2+} electrolytes[13] that a similar broad endothermic peak either may be associated with the presence of a PEO/salt complex poorly defined chemically or can be explained by a process of melting and gradual dissolution of salt-rich complex compositions in the PEO amorphous phase.

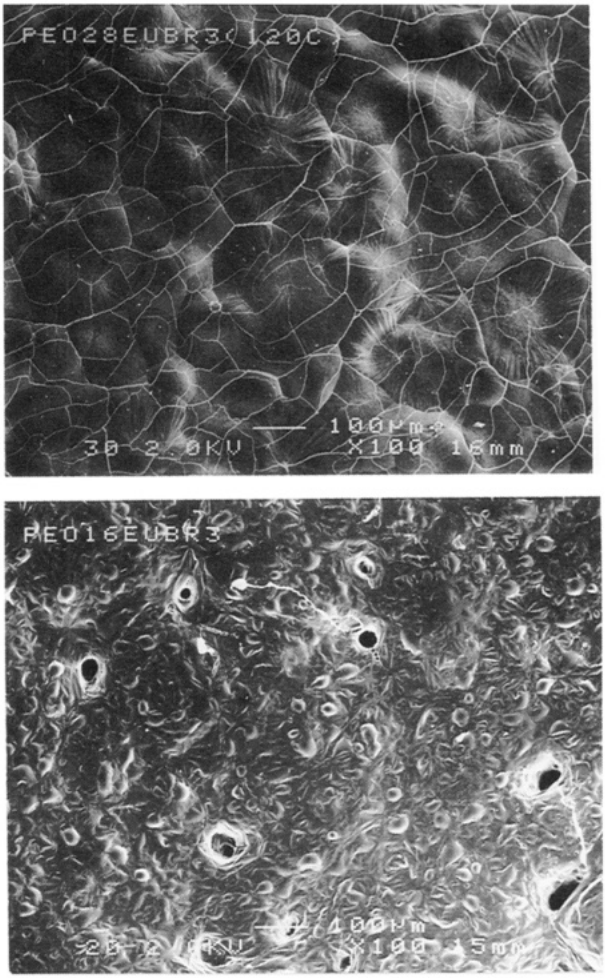

Figure 3. SEM micrographs for (a, top) $PEO_{28}EuBr_3$ and (b, bottom) $PEO_{16}EuBr_3$ at 100×. Note that composition $n = 28$ was dried at $T = 120$ °C.

It is observed from the DSC data (Figure 1) that the intensity of the PEO melting endotherm decreases with increasing salt concentration. This is interpreted as being due to the variation of the ratio of crystalline vs amorphous material. This observation is consistent with microscopy analysis. Figure 3 illustrates the morphology at room temperature of PEO_nEuBr_3 films with composition $n = 28$ (Figure 3a) and $n = 16$ (Figure 3b) as obtained by SEM. It can be seen that the electrolytes are partially crystalline at room temperature and spherulites are clearly visible, which is consistent with previous studies of PEO-based electrolytes.[7] No evidence of salt-free regions was observed with EDX compositional analysis and X-ray distribution maps, which indicates that the spherulites consist of PEO and salt mixtures. Low salt concentration electrolytes such as $PEO_{40}EuBr_3$ show large and well-defined spherulites. The size of the spherulites decreases with increasing salt concentration. This is due to an increase in the amount of amorphous material, which reduces the rate of crystalline of the polymer and hinders spherulite growth.[34] Similar results were obtained with optical microscopy. The morphology of the film $n = 16$ at room temperature (Figure 3b) shows two different crystalline regions. The smaller areas are brighter and appear to be associated with a high-melting-point crystalline

(33) Armand, M. B.; Gauthier, M. *High Conductivity Solid Ionic Conductors—Recent Trends and Applications*; Takahashi, T., Ed.; Word Scientific Press: Singapore, 1989; p 115.

(34) Cope, B. C.; Glasse, M. D. *Electrochemical Science and Technology of Polymers*; Linford, R. G., Ed.; Elsevier Applied Science: London, 1990; p 233.

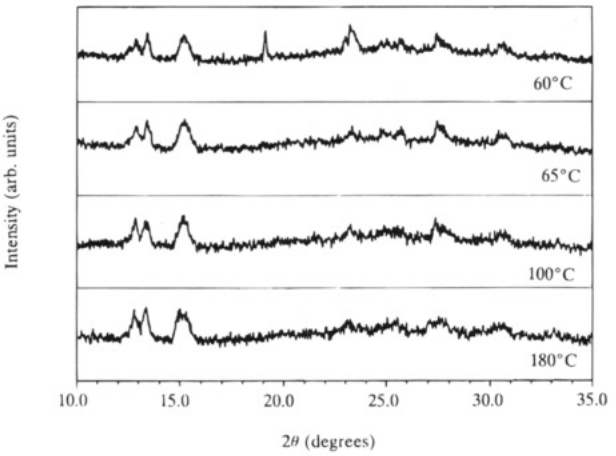

Figure 4. X-ray diffraction pattern of $PEO_{16}EuBr_3$ at 60, 65, 100, and 180 °C.

complex. The larger areas consist of poorly defined and faint spherulites. The formation of faint salt-rich spherulites results from a slower crystallization process.[34] These spherulites have lower crystallinity and are associated with a lower intensity DSC peak (Figure 1) and, as mentioned above, may result from the coexistence of crystalline PEO and an eutectic phase of a PEO−PEO/salt complex. Upon heating, the spherulites in the films $n \geq 16$ were seen to melt within the temperature range 61−68 °C. This is characterized by an intense color change and corresponds to the sharp first endotherm seen in the DSC curves (Figure 1). Films with $n \leq 8$, however, only showed a slight color brightening around 65 °C. No significant structural changes could be detected with further increase in temperature. A gradual darkening of the films was observed between 80 and 100 °C probably due to the loss of water. At temperatures around 130−140 °C, the electrolytes were seen to change from rubbery to liquidlike, which is consistent with other reports.[20,22] This process was observed to occur within the temperature range 10−30 °C depending on the film composition. Incomplete melting was observed for film $n = 16$, suggesting the presence of a high-melting salt-rich polymer−salt complex with a melting point above the onset of PEO decomposition. This result is supported by X-ray analysis. Figure 4 shows the XRD pattern of $PEO_{16}EuBr_3$ taken with increasing temperature (60, 65, 100, and 180 °C). It can be seen that the diffraction peaks corresponding to crystalline pure PEO disappear between 60 and 65 °C as PEO melts, but a crystalline complex is still observed at 180 °C, which agrees well with the incomplete melting observed by microscopy.

No evidence of any spherulitic structure was detected at room temperature for films with compositions $n \leq 8$, as illustrated in Figure 5 for PEO_3EuBr_3. This result agrees well with the results obtained from DSC analysis (Figure 1), which show the formation of a high-melting-point crystalline complex with a stoichiometry close to 3:1 for salt-rich films. These salt-rich Eu^{3+}-based electrolytes are glassy, transparent, and fragile films when no traces of water are detected. The glass transition temperature, T_g, for PEO_3EuBr_3 and PEO_4EuBr_3 films was found to be above room temperature within the temperature range 42−47 °C. This sharp temperature increase relatively to the T_g of pure PEO (≈−60 °C) can be explained by a simultaneous strong interaction between the cations and ether oxygens of different chains, which leads to the formation of transient inter- and/or intramolecular cross-links that significantly reduce chain mobility.[13,26,35−37] In fact, recent studies by Bruce[38] in salt−polyether systems where the oxygen−cation ratio is approximately 4:1 or 3:1 have suggested that preferential formation of intrachain cross-links are responsible for stiffening of the chains and, consequently for the sharp increase observed in T_g. These cross-links introduce a local compression and an ordering effect of the polymer matrix and, in general, for high salt concentrations the complexes comprise essentially a single phase, amorphous[13,35,36] or crystalline.[38] In particular, the analysis reported by James et al.[36] on highly concentrated PPO complexes led to the conclusion that optical transparency and high T_g values are associated with the formation of a single phase. The physical characteristics of salt-rich Eu^{3+} electrolytes, $n = 3, 4$, namely, their transparency and glassy behavior, and the DSC, XRD, and SEM results seem to corroborate this conclusion.

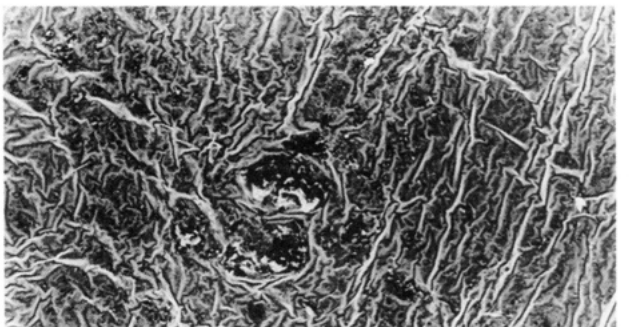

Figure 5. SEM micrographs for PEO_3EuBr_3 at 100×. The structures observed in the middle of the figure result from a nucleation of different impurities as the EDX microanalysis has shown.

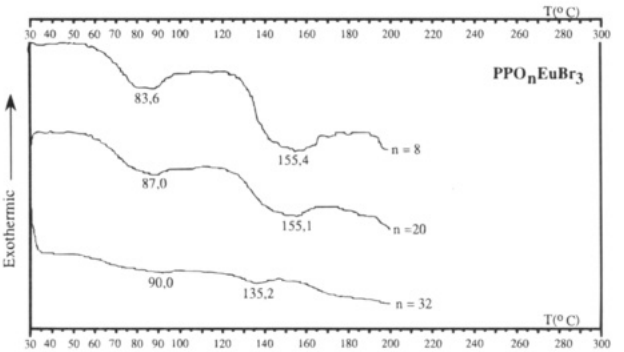

Figure 6. DSC curves for the first heating cycle of the system PPO_nEuBr_3 with n ranging from 32 to 8. (Films with $n \geq 20$ were run at 10 °C/min and the film with $n = 8$ was run at 5 °C/min.)

As mentioned previously, selected compositions of PPO_nEuBr_3 were also studied. Figure 6 shows the DSC curves obtained during the first heating cycle of PPO_nEuBr_3, $n = 32, 20, 8$. It can be seen that a high-melting complex is also formed for salt-rich PPO−Eu^{3+} electrolytes. No evidence of salt precipitation from the polymer

(35) Wetton, R. E.; James, D. B.; Whiting, W. *J. Polym. Sci., Polym. Lett. Ed.* **1976**, *14*, 577.
(36) James, D. B.; Wetton, R. E.; Brown, D. S. *Polymer* **1979**, *20*, 187.
(37) Vincent, C. A. *Electrochemical Science and Technology of Polymers*; Linford, R. G., Ed.; Elsevier Applied Science: London, 1990; p 47.
(38) Bruce, P. G. *Electrochim. Acta* **1995**, *40*, 2077.

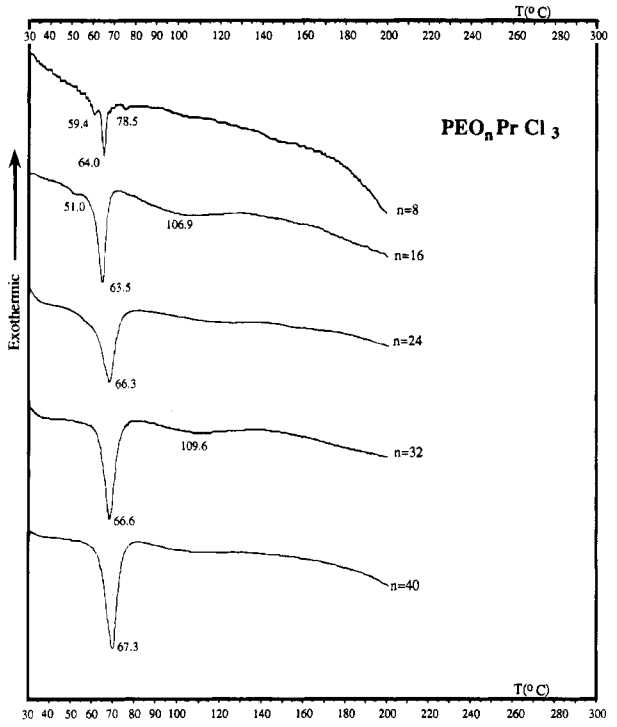

Figure 7. DSC curves for the first heating cycle of the system PEO_nPrCl_3 with n = 40 to 8. Note the different scale of the DSC curve of film PEO_8PrCl_3.

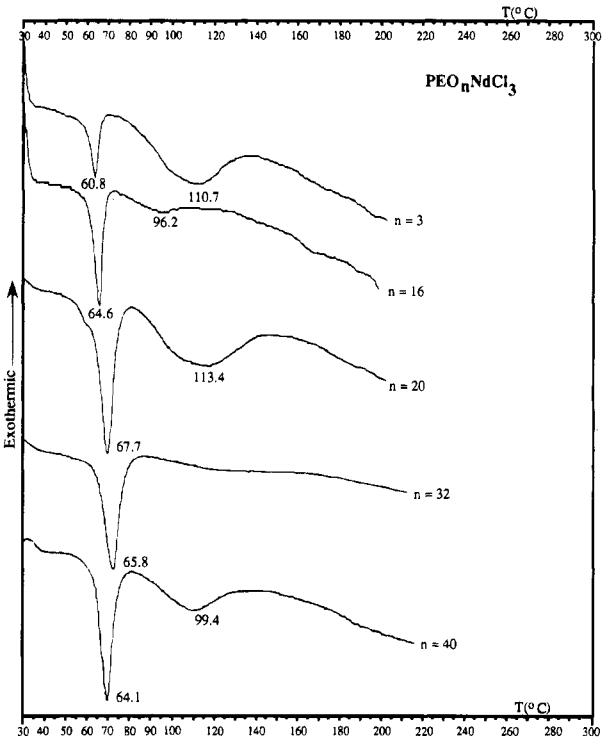

Figure 8. DSC curves for the first heating cycle of the system PEO_nNdCl_3 with n ranging from 40 to 3. (Films with $n \geq 20$ were run at 10 °C/min and films with $n \leq 16$ were run at 5 °C/min.)

was detected for the PPO samples in the temperature range used. This indicates that the broad endotherm observed between 140 and 160 °C (Figure 6) is not the result of a salting-out effect as reported previously for other PPO–salt systems.[39,40] Therefore, we believe that a high-melting complex poorly defined chemically is formed for salt-rich PPO-Eu^{3+} electrolytes. However, the formation, structure, and crystallinity of this complex phase are still unclear.

PEO_nPrCl_3 and PEO_nNdCl_3 Systems. Selected compositions of Pr^{3+}- and Nd^{3+}-based PEO electrolytes were also studied. Figures 7 and 8 show the DSC curves obtained during the first heating cycle of PEO_nPrCl_3, n = 40, 32, 24, 16, 8, and PEO_nNdCl_3, n = 40, 32, 20, 16, 3, respectively. As observed previously for the Eu^{3+}-based electrolytes, the temperature of the first endotherm is close to the melting point of pure PEO, thus indicating the presence of uncomplexed crystalline PEO in the crystalline phase of the films.

From Figures 7 and 8, it can be seen that the intensity of the first endotherm decreases with increasing salt concentration, which results from a variation in the fraction of crystalline vs amorphous material. This is consistent with the results obtained from microscopy analysis. Figure 9 illustrates the morphology at room temperature of the films $PEO_{40}PrCl_3$, PEO_8PrCl_3, and $PEO_{40}NdCl_3$ as obtained by SEM. Well-defined and large spherulites with brightly transmitting regions are observed for the composition n = 40 (Figure 9a,c). The spherulites appear to be larger in the Pr^{3+} system. The size of the spherulites decreases for salt-rich compositions as more amorphous material gets incorporated in the crystalline PEO phase. No visible evidence of a crystalline PEO phase was detected for PEO_8PrCl_3 at room temperature (Figure 9b). These results are consistent with those observed for the PEO–Eu^{3+} system.

For the films with higher salt concentration, $n \leq 16$, the temperature of the first endotherm shifts to a lower value due to an increase of the amount of dissolved ions being incorporated in the crystalline PEO phase. The Pr^{3+}-based electrolytes show an additional smaller peak adjacent to the first endotherm (Figure 7) which did not occur during the reheating cycle. These results are similar to those observed for the Eu^{3+}-based films, indicating again that both uncomplexed crystalline PEO and the eutectic phase of a PEO–PEO/salt complex are present at room temperature for these compositions. The presence of this eutectic phase in the Pr^{3+}-based electrolytes (Figure 7) is probably associated with a stoichiometric high-melting-point crystalline complex similar to that observed for Eu^{3+}-based electrolytes. On the other hand, for salt-rich Nd^{3+}-based electrolytes (Figure 8) there is no evidence of an eutectic phase, which indicates that a high-melting-point crystalline complex with a well-defined stoichiometry is not formed for Nd^{3+}-rich compositions. These Nd^{3+}-based films (Figure 8) show, in addition, a broad endotherm around 100–110 °C, which probably results from the loss of water eventually adsorbed during sample transport. However, as with the Eu^{3+}-based system, it either may be associated with the presence of a PEO/salt complex poorly defined chemically or can be attributed to a process of melting and gradual dissolution of salt-rich compositions of PEO-salt complexes into the amorphous phase. This broad endotherm is not as evident for the $PEO_{32}NdCl_3$ electrolyte and for the Pr^{3+}-based films (Figures 7 and 8).

Conclusions

DSC, polarized microscopy analysis, SEM/EDX, and X-ray diffraction studies were performed on samples of

(39) Teeters, D.; Frech, R. *Solid State Ionics* **1986**, *18/19*, 271.
(40) Greenbaum, S. G.; Pak, Y. S.; Wintersgill, M. C.; Fontanella, J. J.; Schultz, J. W.; Andeen, C. G. *J. Electrochem. Soc.* **1988**, *135*, 235.

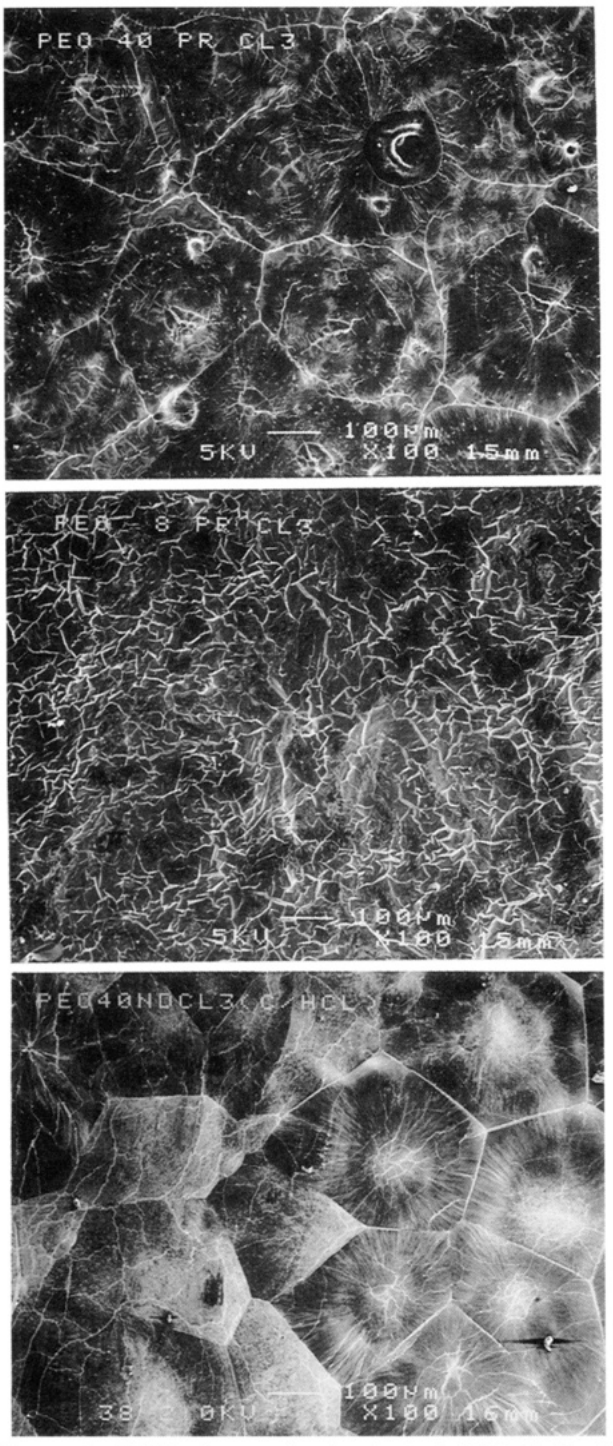

Figure 9. SEM micrographs for (a, top) $PEO_{40}PrCl_3$, (b, middle) PEO_8PrCl_3, and (c, bottom) $PEO_{40}NdCl_3$ at 100×.

PEO_nEuBr_3, PEO_nNdCl_3, and PEO_nPrCl_3 complexes with values of n ranging from 80 to 3. Several observations can be drawn from these analysis and are as follows:

The morphology of PEO-lanthanide based electrolytes with $80 \geq n \geq 16$ at room temperature, consists of mixtures of spherulitic crystalline regions interspersed by amorphous solutions of salt in PEO. Electrolytes with low salt concentrations, $n \geq 32$, have large and well-defined spherulites. These spherulites appear to be larger for the Pr and Nd systems as compared to the Eu system. The size of the spherulites decreases with increasing salt concentration due to the variation of the ratio of crystalline PEO vs amorphous material as revealed by DSC, polarized microscopy, SEM/EDX, and XRD analysis. Europium and praseodymium films with $16 \geq n \geq 8$ show two different crystalline phases at room temperature, whereas the same neodymium compositions only show one crystalline phase.

Detailed DSC measurements carried out in the temperature range 25−300 °C have shown that all the Pr^{3+} and Nd^{3+} films as well as Eu^{3+} PEO-based electrolytes with $n \geq 12$ exhibit an endothermic peak around 65 °C which is associated with the melting of crystalline PEO. The actual value of this peak varies with composition due to incorporation of some of the salt in the crystalline PEO phase. Europium and praseodymium salt-rich films with compositions between $n = 16$ and $n = 7$ showed, in addition, a small endothermic peak around 60 °C, adjacent to the PEO melting endotherm. This smaller endothermic peak results from the eutectic phase of PEO and PEO/salt complex. Initial results for Eu^{3+} electrolytes indicate that the eutectic composition lies within $12 > n \geq 8$. The presence of this eutectic phase is probably associated with a stoichiometric high-melting-point crystalline complex. In fact, in the case of Eu^{3+}-based electrolytes this crystalline complex was distinctly observed for salt-rich electrolytes with a stoichiometry close to an oxygen−cation ratio of 3:1. On the other hand, the morphology of the Nd^{3+}-based electrolytes was found to be independent of the salt concentration and there is no indication of a stoichiometric crystalline complex. In addition, most of the PEO−lanthanide based electrolytes showed a broader endotherm at ≈100−110 °C, which might be due to the loss of water, to the presence of a PEO/salt complex poorly defined chemically or to a gradual melting of PEO/salt complexes.

A salt-rich phase is also observed for the PPO_8EuBr_3 electrolyte but its structural nature is yet unclear.

Acknowledgment. The authors would like to express their gratitude to Jie Shi at the University of St. Andrews, UK, for his valuable technical assistance and help in running the X-ray analysis. They also acknowledge Antonieta Ribeiro at the Instituto Superior Técnico of Lisbon, Portugal, for her cooperation in the electrolytes preparation and in the DSC measurements. This work was financed by FEDER and JNICT, STRIDE program, Portugal, STRDB/C/CTM/628/92.

CM950205K